Mater. Res. Soc. Symp. Proc. Vol. 991 © 2007 Materials Research Society 0991-C06-03

Micromachined Shear Stress Sensors for Characterization of Surface Forces during Chemical Mechanical Polishing

Andrew Mueller[1], Robert White[1], Vincent Manno[1], Chris Rogers[1], Sriram Anjur[2], and Mansour Moinpour[3]
[1]Mechanical Engineering, Tufts University, 200 College Ave, Medford, MA, 02155
[2]Cabot Microelectronics, Aurora, IL, 60504
[3]Intel Corporation, Santa Clara, CA, 95052

ABSTRACT

This paper describes the fabrication and calibration of micromachined shear stress sensors intended for characterization of the local pad-wafer contact forces present during chemical-mechanical polishing. Sensors consist of arrays of microfabricated poly-dimethyl-siloxane (PDMS) posts and are able to measure forces ranging from 2 to 200 μN. The posts are 100 μm high and have diameters of 40-100 μm. Calibrated post deflection sensitivities are linear and lie between 0.2 μm/μN and 1.3 μm/μN. Sensor design, fabrication, and calibration are detailed. Feasibility is established for sensor integration into a CMP scale model test setup, including an optical viewing method for observing post deflection during polishing. Initial micrographs of post deflection during polishing do not yet have sufficient resolution to determine the microscale forces during polishing.

INTRODUCTION

As feature sizes in the semiconductor industry continue to shrink, the importance of planarizing substrates both globally and locally grows. Chemical mechanical planarization (CMP) is now the foremost nanomanufacturing process worldwide. It has an annual economic impact over $1 billion and individual CMP processes are well established within certain enterprises. Still, the ability to change CMP parameters and predict the effect this will have on material removal rates is not yet realized [1, 2]. The CMP process is widely used and removal rates for certain systems have been characterized experimentally in terms of many of the polishing parameters [3], but a comprehensive model involving all variables and their effects on material removal rate and non-uniformity is lacking.

The interfacial shear force between polishing pad and substrate is one of the many variables in the CMP process that has previously been studied in order to gain further understanding of the polishing model [4, 5]. These shear forces are an important parameter in CMP as they have a direct influence on material removal rates, processing temperature variations, and failure modes. Investigating local (micro scale) and global (coefficient of friction) shear forces *in situ* captures stick-slip phenomena and other vibration modes that time-averaging techniques or post polishing analysis cannot [6]. Sensors developed for determining these shear forces must remain unaffected by the chemical slurry present during CMP (as well as the mechanical polishing process itself) and be able to provide *in situ* data from the pad-substrate interface.

Previous studies of CMP shear forces focus on *in situ* global (friction) forces obtained experimentally [6, 7], *ex situ* local forces obtained experimentally [8], or *in situ* local forces obtained by modeling and CMP theory [3]. This paper describes the fabrication and implementation of a micromachined shear stress sensor for determining the local *in situ* shear forces present during CMP. The sensor is based on arrays of cylindrical posts that deflect due to the influence of shear forces. Other authors have reported using similar microfabricated pillar designs to sense shear forces due to solid interactions [9] as well as fluid interactions [10] in other applications. However, to the best of the authors' knowledge no one has obtained CMP shear force measurements using such sensors.

As shear force is determined optically, the sensor does not need to transmit electrical signals and thus operates well in the conducting slurry. Calibration of the sensors is detailed and the process for integrating the sensor is illustrated. The current system incorporates multiple devices with displacement sensitivities of 0.2 μm/μN to 1.3 μm/μN. These sensitivities were designed based on estimates of individual asperity forces in the range of 4-400 μN. Such forces will result in measurable deflections. Experimental characterization of post stiffness and computational models of expected post stiffness are in good agreement. A linear elastic constitutive law is sufficient for the structure. Nonlinear geometric effects due to large deflections and full three dimensional displacement fields are needed to accurately model structure response.

EXPERIMENTAL DESIGN

The sensor developed here will be incorporated with related CMP modeling research being conducted at Tufts University [4-7]. Accordingly, one of the primary design parameters was that the sensor array must integrate with the established CMP setup detailed in [6]. The PDMS sensor presented in this paper replaces the wafer in the polishing setup, and is designed for use with a stiff polishing pad, specifically the Rodel IC1000. Although the following sections describe the sensor design and testing explicitly using this pad, a corresponding sensor for use with a soft pad could be designed using identical methods.

Design

The microfabricated posts in the shear sensor are made of polydimethylsiloxane (PDMS), a mechanically and chemically robust polymer. The use of PDMS for sensor applications has many advantages over other materials. PDMS is very inexpensive, flexible, and easily fabricated. It is stable at high and low temperatures, impermeable to water, and permeable to gases [11]. PDMS is also transparent. This is a crucial property for our application, as it allows deflections of posts at the sensor-pad interface to be obtained optically through the back of the wafer. No interconnects are necessary, which is ideal when working in the CMP environment where electrical connections on the wafer could easily be disrupted by the mechanical and chemical processes.

Figure 1 shows a cartoon of how the PDMS posts react to asperities 'polishing' the sensor. The image on the right shows the basic unit of the shear stress sensor presented here: the recessed micro post with bulk PDMS surrounding it. Nearly 98% of the wafer surface is planar

PDMS, it is only occasionally broken by the annular well region around a sensor post. This allows the majority of the normal force to be carried by the bulk PDMS thus not compressing or buckling the sensor posts. Measured forces remain primarily lateral shear forces. The post and well are both circular, enabling shear force detection in both in-plane directions.

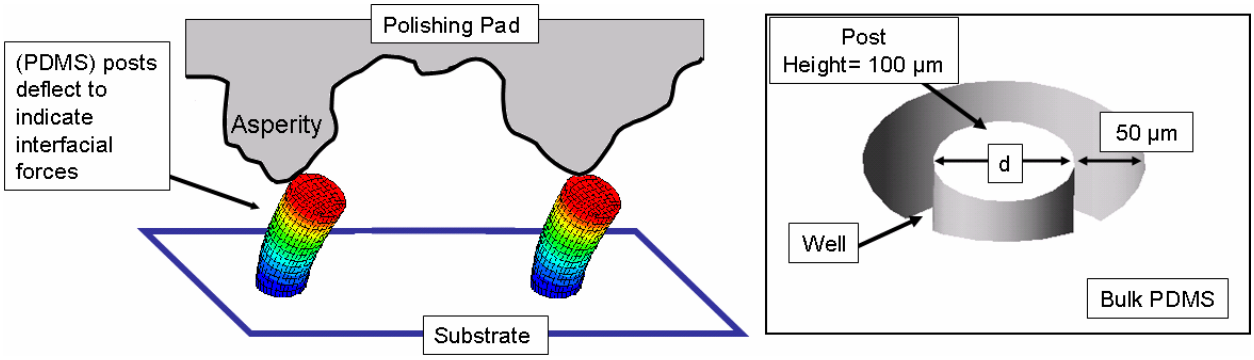

Figure 1: PDMS posts deflect due to shear forces. The basic unit of the shear stress sensor is the recessed micro post (right image). An array of posts with as-designed height 100 microns, and varying diameter, d, have been designed and fabricated.

Post design is based off of estimates of shear forces present while polishing a 4" wafer using an IC1000 pad with an applied pressure of 1.7psi. Coefficient of friction (CoF) values of 0.30 (+/- 0.03) have been obtained under these conditions from previous work at Tufts. The total shear force on the wafer is thus approximately 30 N. At an applied pressure of 1.7 psi in a static situation, an IC1000 pad will contact only approximately 0.7% of the wafer through pad asperities [12]. At this static pressure, the mean radius of contact between a single asperity and the wafer is approximately 5µm (estimated from [12]). Based on these estimates, the wafer will be in contact with approximately 700,000 asperities. With a total shear force of approximately 30 N, the mean force delivered by an asperity is expected to be on the order of 40 µN. The shear sensors have been designed to handle a range extending one order of magnitude above and below this mean, from 4-400 µN.

Fluid shear forces during CMP due to the slurry-wafer interactions were also considered. Three dimensional numerical modeling of the sensor-slurry system using incompressible, viscous, nonlinear Navier-Stokes with 0.5 m/s inlet velocity and rigid sensor structures indicated that fluid shear forces are less than 1µN. This agrees well with other CMP models which sometimes omit fluid shear forces as negligible in force computations [13]. It is therefore expected that fluid shear forces will not contribute significantly to the deflection of the posts.

The size of the post structures must be selected to produce measurable deflections over the estimated range of asperity forces. In addition, our experimental work on PDMS casting using an SU-8 mold indicated that the aspect ratio of the posts should be kept below approximately 4:1 (height:diameter). Euler-Bernoulli beam theory was used to obtain a range of PDMS post diameters that will deflect between 5 µm and 50 µm when reacting to shear forces from 4 µN to 400 µN. The material is modeled as elastic and the modulus used is 750 kPa, the appropriate value for a 10:1 mixture of PDMS base to curing agent [14]. Based on this analysis, the range of diameters for the post array was selected as 30 µm to 100 µm, meeting the sensitivity and dynamic range goals. This size also allows reasonable in-plane spatial resolution

for the sensor. Our goal is to be able to resolve a single asperity passing during polishing; we estimated the spacing between asperity contacts to be on the order of 30 μm.

Table I shows the posts used in the sensor array, their expected stiffnesses, and the resulting deflections from estimated asperity forces. As the table shows, an asperity force on the low end of the expected range, 4 μN, deflects the smallest post by approximately 50μm. Similarly, an asperity force on the high end of the expected range, 400 μN deflects the largest post approximately 50μm as well. Actual asperity forces are expected to fall mainly in this range; thus all sensors will be useful in determining shear stresses present. Each array measures 2 mm by 1.5 mm in area. The arrays are repeated over the wafer with a spacing of approximately 10 mm.

Table I. Estimated sensitivity of sensor posts based on linear beam theory. Post length = 100μm, elastic modulus = 750 kPa

Post Diameter(μm)	30	40	50	60	70	80	90	100
Estimated Compliance (μm/μN)	14.25	4.51	1.85	0.89	0.48	0.28	0.18	0.12
Minimum Estimated Deflection for a force of 4 μN (μm)	57.0	18.0	7.4	3.6	1.9	1.1	0.7	0.5
Maximum Estimated Deflection for a force of 400 μN (μm)	5700.8	1803.8	738.8	356.3	192.3	112.7	70.4	46.2
Asperity Forces: 4-400μN								

Fabrication

All processing is conducted in the Tufts Micro- and Nanofabrication Facility (TMNF). Sensors are fabricated through a modified two-layer PDMS micromolding process similar to that described in [15]. In this process a master consisting of two layers, one silicon dioxide and one SU-8 photoresist, is microfabricated and used as a mold for the PDMS sensor structures. A single master mold can be used to create multiple copies of the full wafer PDMS sensor array.

The starting substrates are 100 mm diameter, <100> oriented, p-type 1-10 Ω·cm (boron) silicon wafers with 1μm of silicon dioxide, grown by wet thermal oxidation. 1 μm of SPR220-3.0 positive photoresist (Rohm & Haas) is spun on and used as a mask for a buffered hydrofluoric acid etch (Ultratech NP 13:2) of the oxide. The etch creates the indicator numbers and deflection notches (as shown in Figure 3) in the 1μm oxide layer. Lithography is repeated with a second mask using the negative tone, high aspect ratio epoxy photoresist SU-8-100 (MicroChem Corp.). The SU-8-100 is spun at 500 rpm for 50 seconds and 3000 rpm for 1 minute, prebaked at 65°C for 15 minutes and 95°C for 32 minutes. The exposure dose is 300 mJ/cm^2 at I-line. A post exposure bake of 65°C for 1 minute and 95°C for 10 minutes is used followed by a 10 minute develop in PM Acetate developer. This results in an approximately 100-140 μm thick SU-8 structure, which, along with the thin patterned oxide, is used as the master mold for the PDMS.

The master mold is silanized in a rough vacuum desiccator with 2 to 3 drops of the silanizing agent tridecafluoro tetrahyroctyl trichlorosilane for 1.5 hours. A 10:1 PDMS ratio of base to curing agent is mixed (Dow Corning Sylgard 184), degassed in a rough vacuum chamber, and poured over the silanized master mold. The PDMS is cured in place on the master mold on a

hot plate at 60°C for 4 hours. It can then be peeled from the mold. The PDMS structure is bonded to a Pyrex wafer (Corning type 7740 Pyrex glass) by exposing both surfaces to a 200 mT, 25 W oxygen plasma for 30s, placing the PDMS and glass in contact, and heating on a hotplate at 60 °C for 15 minutes.

Calibration

Sensor calibration is carried out using a microscale mechanical testing technique, called MAT-Test, developed by Hopcroft et al [16]. The technique utilizes a contact surface profilometer to obtain force deflection curves for small structures. To determine the stiffness of the PDMS sensing posts, calibration posts (not recessed in wells) are fabricated as shown in the left image of Figure 2. The posts shown are 80μm in diameter and the dashed line indicates where the sensor is cut so that the posts lay horizontally for the profilometer testing, as shown in the right image. In this fashion, the force deflection curves obtained indicate the stiffness of the PDMS post tested. A Veeco Dektak 6M Stylus Profilometer is used to supply downforces between 10-150 μN. The resulting deflections are measured by the tool. Notice the range of possible downforces falls within the estimated asperity force range (4-400 μN).

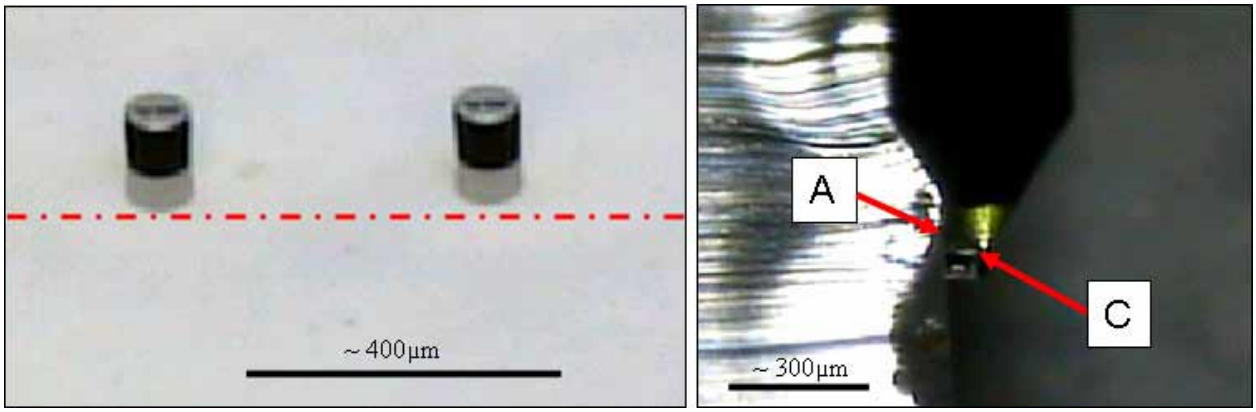

Figure 2: Left: Perspective microscope images of calibration posts used for stiffness testing. 80um diameter posts are shown. The dashed line indicates where the PDMS sensor is cut so that it lays horizontally for calibration with the stylus profilometer. Right: Perspective microscope image showing the stylus profilometer stylus tip pressing on the end of a post. This is the configuration used for stiffness calibration. 'A' and 'C' indicate the edge of the PDMS slab and the end of the post, respectively.

Integration

The calibrated sensor is integrated into the current CMP setup shown in [6]. The sensor wafer replaces the substrate being polished. The posts are oriented downward, with the tips in contact with the polishing pad. To mate the sensor with the CMP axel and secure it during polishing, an acrylic mating plate is glued to the back of the Pyrex wafer which carries the PDMS structures. The acrylic plate has four large viewing windows cut through it to allow the posts to be observed optically through the back side of the Pyrex and PDMS. A high resolution color CCD camera is coupled to a 15 X relay lens and a 10 X microscope objective to determine

post deflection during CMP. Camera resolution and speed is 3.2 megapixels and 14frames per second, respectively. Pixel size is approximately 2μm on a side. Light is provided through a fiber optic light guide. During the shear force experiments presented here, the sensor wafer remains stationary as the polishing pad rotates below it. In the future, we intend to increase the camera capture rate and rotate both wafer and pad simultaneously.

Industrial polishing parameters are adjusted to account for laboratory research scaling [6]. The slurry used is a 3:2 water dilution of Cabot Microelectronics' Cab-O-Sperse SC-1 3.1 wt% abrasive. The laboratory CMP equipment is scaled down from an industrial CMP system by a factor of 2. A summary of adjustments is supplied in [6].

RESULTS AND DISCUSSION

Fabrication

The sensor was successfully fabricated. Microscope images are shown in Figure 3. All indicator numbers and deflection notches (1μm thick) resolved well. The SU-8-100 master mold exhibited some variation in thickness across the wafer, varying from 125-140 μm. The length of the posts is determined by this thickness. It is therefore important that the location of a particular post is known so that its length, and hence its sensitivity to applied force, can be known. The 100 μm through 40 μm diameter posts resolved well. The 30μm diameter posts did not fully resolve in all cases.

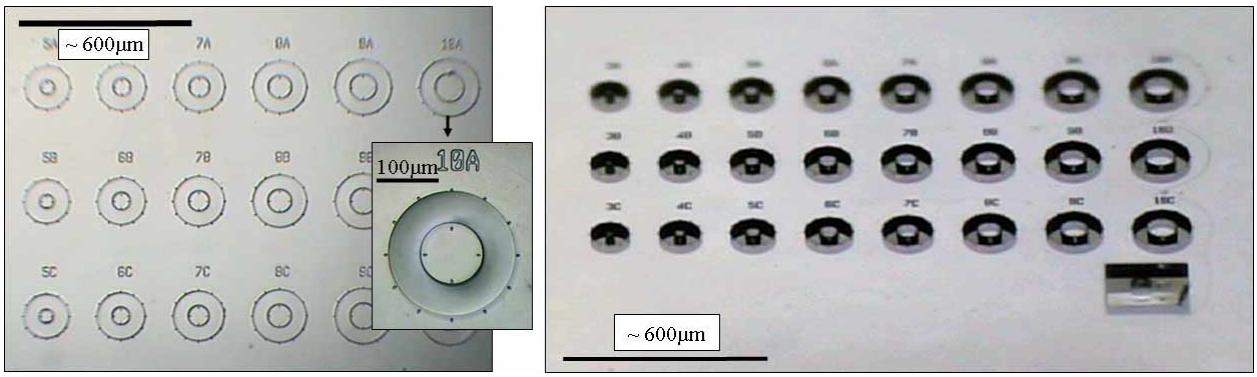

Figure 3: Microscope images of the sensor array. Left: top-down light microscope image. The inset clearly shows the tick marks fabricated on the post and around the well edges. These tick marks are intended to assist in determination of post tip deformation during polishing. Right: An angled perspective light microscope image shows the three dimensional structure of posts in wells.

Calibration

In Figure 2, above, a photograph of the geometry of the profilometry calibration is shown. The PDMS structure has been sectioned and turned on its side, so that the posts are now cantilevered out. The stylus tip travels from left to right in the image. Figure 4, below, shows

the results of a typical profilometry scan. Letters have been placed in both the photograph and the scan data to show the sequential events that occur during the scan. Initially, the tip travels along the supporting PDMS slab (which had been sectioned using a razor blade). It reaches the end of the PDMS slab (location A) and drops down onto the post (location B). The tip then travels along the post, deflecting the post. Various downforces can be used, resulting in various degrees of post deflection. The stylus tip eventually reaches the end of the post (location C) and the stylus begins to drop off of the post. The stylus tip has a radius of 12.5 µm, so 12.5 µm after reaching the end of the post, the stylus starts to drop very rapidly (location D). The post deflection sensitivity in response to the stylus force can be determined by plotting the measured deflection of the post against the applied force.

Results from five identical profilometer scans along a 90µm diameter calibration post at a downforce of 10µN are also shown in Figure 4. Consecutive scans agree well with each other; all post deflection appears to be purely elastic.

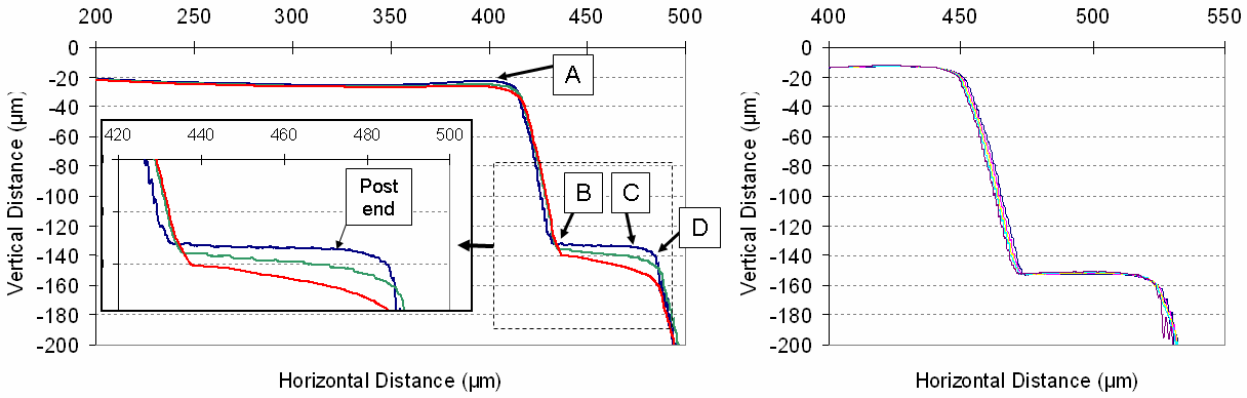

Figure 4: Left: Stylus profilometer scans of a 120 µm long, 100 µm diameter post using downforces of 10, 30, and 50 µN. Note that as the force is increased, the deflection increases. The inset indicates the end of the post. Right: Five profilometer scans of a PDMS post show repeatable deflection results and no plastic deformation.

Post deflection is determined by plotting downforce vs. stylus vertical position and then applying a vertical position offset to the curve to force it to pass through the 0 µN, 0 µm point. This vertical position offset is required since the vertical distance measured by the stylus profilometer is referenced to an arbitrary zero point. Downforce is limited to 50µN to ensure that the horizontal distance measured by the profilometer approximately reflects distance along the post. Figure 5 shows deflection vs. applied force for the 40 µm and 100 µm diameter posts. All calibration and model results are reported at a location 100 µm from the base of the post. This location is selected because it is the designed post length and ensures that the stylus tip remains on the post during scans. The displacement sensitivity (compliance) is 1.3 µm/µN (± .08 µm/µN) for the 40 µm diameter post and 0.23 µm/µN (± .02 µm/µN) for the 100µm diameter post. Sensor deflection vs. applied force is linear over the range of applied forces.

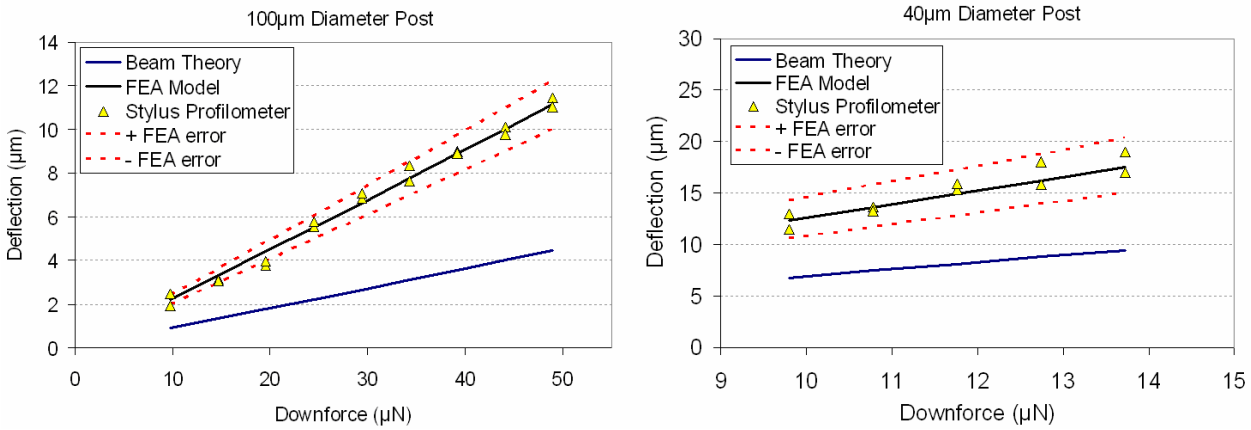

Figure 5: Force-deflection curves for the smallest and largest diameter posts calibrated. The results of Euler-Bernoulli beam theory models, and three dimensional linear elastic finite element analysis (FEA) models are included. The dashed lines indicated the FEA model results when ±5% is added to the length of the post.

The stylus profilometry calibration data agrees well with a three dimensional finite element model. The FEA results shown in Figure 5 are produced using Abaqus ™ finite element analysis software. Figure 6 shows the model mesh and boundary conditions used when analyzing a 100 µm long, 100 µm diameter post. The C3D8R element, an eight node, linear, reduced integration continuum stress/displacement brick element with hourglass control, is used. This element uses a linear isotropic material model. An elastic modulus of 750 kPa and a Poisson ratio of 0.5 is selected based on the measurements given in [14] for a 10:1 base to curing agent ratio of the Dow Corning Sylgard 184 PDMS formulation. Nonlinear large deflection geometric effects are included in the computation, as the deflections of the structure are a significant fraction of its dimensions. Compliance of the PDMS supporting the base of the post is included by meshing and modeling a base region composed of the same material. The base region is 6 times the diameter of the post and 3 times as thick as the post is high. This size for the modeled base region was selected by increasing the size of the modeled base region until the deflection of the tip no longer increased. Essential boundary conditions were used on the bottom of the base region, fixing both displacement and rotation. A distributed shear force was used on the top face of the post with a total integrated force equal to the applied load. The number of elements was increased until the deflection converged. For the model shown in Figure 6, 10025 total elements were used in the mesh.

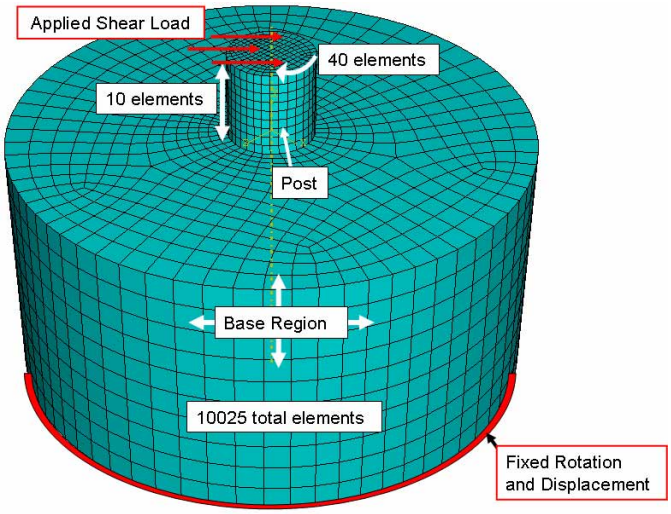

Figure 6. FEA model mesh for a 100 µm tall, 100 µm diameter post. A shear load is applied with the total integral equal to the applied load. Rotation and displacement of the bottom surface are fixed.

Note from the results shown in Figure 5 that the more complex FEA model is needed to predict the observed levels of deflection. A simple Euler-Bernoulli beam model, which was used to design the structures, is not sufficient. For this reason, measured post compliance was approximately twice the designed value. There are three main phenomena included in the FEA simulation which are not in the Euler-Bernoulli beam model but are needed for this particular problem. First, the post is short compared to its width, so the assumptions of Euler-Bernoulli theory are violated. This is addressed by moving to a fully three dimensional elastic solid model. Second, the base of the post is attached to a large slab of PDMS which itself retains significant compliance, contributing to post deflection. The clamped base condition used for the beam theory model was overly stiff in this regard. This issue was addressed by including a compliant base region in the FEA model. Third, the deflections of the post at high forces are large compared to the diameter of the post. This violates linear beam theory. The problem is addressed by including nonlinear geometric effects in the FEA model.

Integration

Figure 7 shows the PDMS sensor wafer integrated into the CMP setup. The camera and fiber optic light sources for observing post deflection are also shown. Preliminary images obtained from this setup are shown in Figure 8. Static images of the sensor wafer in position, but with no slurry and no rotation of the pad, are clear enough to see post deflections in the 5-50 µm range. However, indicator numbers are not easily read and deflection notches cannot be seen at all. This is due to the optical aberrations produced by looking through the Pyrex glass and PDMS. Increased magnification and increased light may improve images. Dyeing of the PDMS surface to increase contrast may also increase post deflection visibility. When slurry is flowing and the pad is rotating, the images become less clear. This can be seen in the right portion of Figure 8. The case shown here was at a low pad speed of 7 rpm and downforce of 0.8 psi Cab-O-Sperse SC-1 slurry diluted at 3:2 with water was used. In this experiment, and in a sequence

of other experiments at rotation rates increasing up to 60 rpm, post tops cannot be adequately distinguished from the surrounding PDMS. Individual post wells are somewhat visible, but deflection readings from the posts cannot yet be reliably obtained.

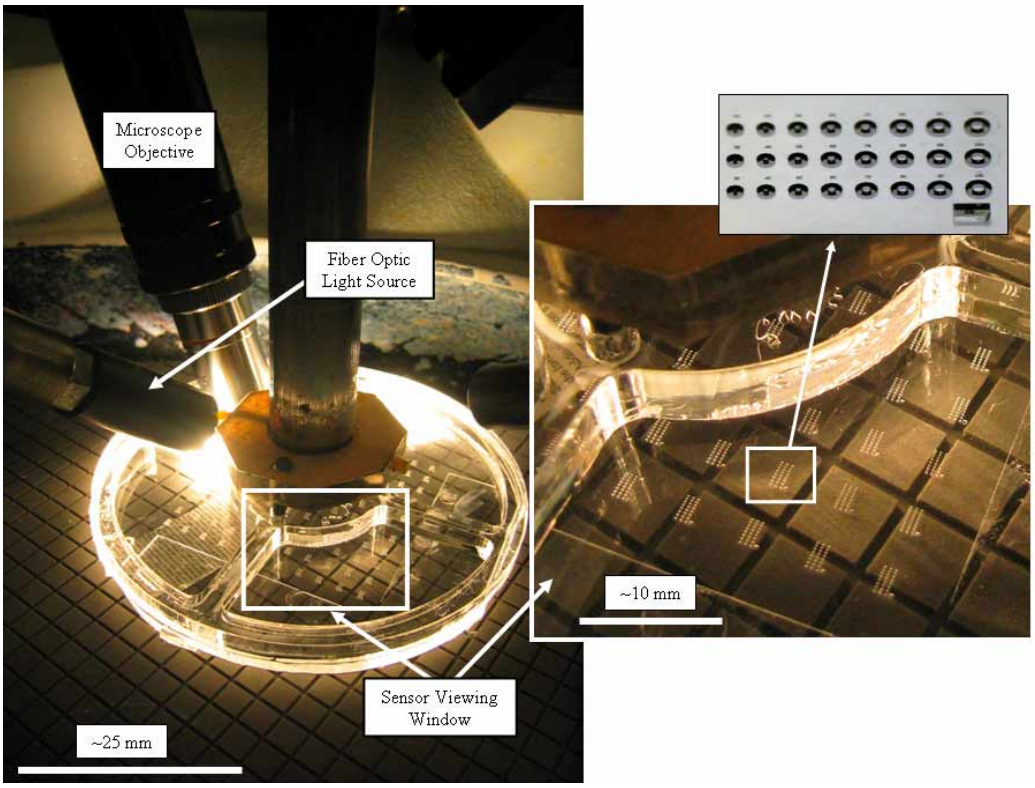

Figure 7: PDMS shear sensor wafer integrated into the CMP setup. The 10 X microscope objective seen in the photography has a working distance of 6 mm. It is coupled to a CCD camera (out of the photograph) with a relay lens. A fiber optic light source is used to illuminate the region of interest.

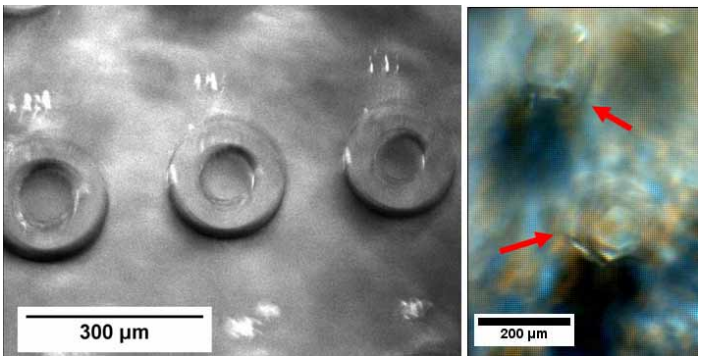

Figure 8: Preliminary images from *in situ* CMP experiments. The left image shows the sensor viewed in place (through the Pyrex wafer and through the PDMS). This image is with no slurry and no pad rotation. The posts and wells are visible, but the small tick marks intended to show post tip deflection can no longer be seen (compare to Figure 3 above). The right image shows the sensor with slurry flowing and 7 rpm pad rotation. The sensor can be seen (indicated by the arrows), but the image is blurred to the point that deflections of the post tip are not yet observable.

CONCLUSIONS

The feasibility of using PDMS micromachined post-in-well shear stress sensors for characterizing of individual asperity forces during CMP has been demonstrated. The sensor arrays consist of 125-140 μm high posts with diameters from 30 to 100 μm. Calibration of the individual posts has been carried out using a stylus profilometer. Results indicate that post deflection is linear in applied force to at least 50 μN. Post stiffness is 1.3 μm/μN (± .08 μm/μN) for the 40 μm diameter post and 0.23 μm/μN (± .02 μm/μN) for the 100μm diameter post. Post deflection appears to be fully elastic, and no permanent deformation has been observed. Post deflection in response to individual asperity forces is expected to be in the range of 5-100 μm. This is based on a 4-400 μN expected asperity shear force range, where the most sensitive post is used for the low end of the range, and the least sensitive post for the high end of the range. Calibrated sensitivities of the post were approximately twice the designed values; due mainly to limitations in the Euler-Bernoulli beam model used in design of the sensor.

The use of a PDMS micromolding process makes fabrication rapid, inexpensive and repeatable. A two layer molding process has been used to include marks on the top side of the sensor posts to aid in deflection visualization. The 40 μm through 100 μm diameter posts were all fabricated successfully. The smallest post, at 30 μm in diameter, was not fully resolved due to the high aspect ratio. A maximum aspect ratio limitation of approximately 4:1 (height:diameter) was established for this process. Post height varied from approximately 120 μm to 140 μm across the wafer due to thickness variations in the SU-8 mold. Further development of mold fabrication will attempt to reduce this variation and meet the 100 μm post height goal.

The sensor structure is transparent, allowing for observation of the posts during polishing through the backside of the wafer. This optical observation method was selected to allow measurement *in situ*. Feasibility has been established for integration of the sensor into the existing scale-model CMP test rig at Tufts University. An optical microscopy setup integrated with the CMP test rig gives approximately 2 μm per pixel, sufficient for viewing the expected levels of deflection.

Initial measurements of sensor structures integrated into the rig demonstrate limitations to the current optical setup which must be overcome to establish measurements of shear forces during polishing. Micrographs of the sensors taken *in situ*, but with no pad rotation and no slurry flowing, demonstrate sufficient resolution. However, when slurry is introduced and rotation of the pad commences, the resolution of the images suffers and post tip deflection cannot be determined.

The limitations present in the current optical setup will be addressed in the future with the intent of achieving measurements of asperity contact forces during polishing. Improvements will be made to the mechanical mounting to reduce camera vibration. A high speed camera will be employed to reduce blurring due to dynamic motion of the structures. Finally, dyeing of the surface of the sensor structures will be attempted to increase contrast and improve our ability to distinguish post deflection.

ACKNOWLEDGMENTS

The authors gratefully acknowledge SRC/Sematech Engineering Research Center for Environmentally Benign Semiconductor Manufacturing for funding this work. We also thank Mr. James Hoffman of Tufts University for his advice and assistance with machining and assembly.

REFERENCES

1. S. H. Ng, C. Zettner, C. Zhou, I. Yoon, S. Danyluk, M. Sacks, and M. Yoda, American Society of Mechanical Engineers, Heat Transfer Division. 374 (3), 199-206 (2003).
2. C. J. Evans, E. Paul, D. Dornfield, D. A. Lucca, G. Byrne, M. Tricard, F. Klocke, O. Dambon and B. A. Mullany, CIRP Annals - Manufacturing Technology. 52 (2), 611-633 (2003).
3. E. Paul, Journal of the Electrochemical Society. 148(6), G355-G358 (2001).
4. J. Lu, J. Coppeta, C. Rogers, V. P. Manno, L. Racz, A. Philipossian, M. Moinpour and F. Kaufman, Materials Research Society Symposium – Proceedings. 2000, E1.2.1.
5. C. Gray, D. Apone, C. Barns, M. Moinpour, S. Anjur, V. Manno and C. Rogers, Materials Research Society Symposium Proceedings. 2004, 165.
6. J. Vlahakis, C. Gray, C. Barns, M. Moinpour, S. Anjur, A. Philipossian, V. Manno and C. Rogers, CMP-MIC Proceedings. 2006.
7. J. Lu, C. Rogers, V. P. Manno, A. Philipossian, S. Anjur and M. Moinpour, Journal of the Electrochemical Society. 151(4), G241-G247 (2004).
8. J. A. Levert and C. S. Korach, Proceedings of the World Tribology Congress III. 427-428 (2005).
9. O. Du Roure, A. Saez, A. Buguin, R. H. Austin, P. Chavrier, P. Siberzan and B. Ladoux, Proceedings of the National Academy of Sciences of the United States of America. 102 (7), 2390-2395 (2005).
10. G. J. M. Krijnen, M. Dijkstra, J. J. Van Baar, S. S. Shankar, W. J. Kuipers, R. J. H. De Boer, D. Altpeter, T. S. J. Lammerink and R. Wiegerink, Nanotechnology. 17 (4), S84-S89 (2006).
11. Dow Corning, www.dowcorning.com, Midland, MI (2007).
12. C. L. Elmufdi and G. P. Muldowney, presented at the 2006 CAMP 9th International Symposium on CMP, Lake Placid, NY, 2006.
13. J. A. Levert, F. M. Mess, R. F. Salant, S. Danyluk and A. R. Baker, Tribol. Trans. 41 (4), 593-599 (1998).
14. D. Armani, C. Liu and N. Aluru, Proceedings of the IEEE Micro Electro Mechanical Systems (MEMS). 1999, 222-227.
15. S. K. Sia and G. M. Whitesides, Electrophoresis. 24(21), 3563-3576 (2003).
16. M. Hopcroft, T. Kramer, G. Kim, K. Takashima, Y. Higo, D. Moore and J. Brugger, Fatigue and Fracture of Engineering Materials and Structures. 28(8), 735-742 (2005).